Charge-Exchange Atoms and Ion Source Divergence in a 20 TW Applied-*B* Ion Diode

A. B. Filuk, J. E. Bailey, A. L. Carlson, D. J. Johnson, P. Lake, T. A. Mehlhorn, L. P. Mix, T. J. Renk, and W. A. Stygar
Sandia National Laboratories, Albuquerque, New Mexico 87185

Y. Maron
Weizmann Institute of Science, Rehovot, Israel, 76100
(Received 29 April 1996)

Space- and time-resolved spectroscopy is used to measure properties of several-keV Li atoms in a 20 TW ion diode. These measurements out in the diode anode-cathode gap are used in a charge-exchange model for the Li atom production in order to obtain the Li^+ beam angular divergence within 50 μm of the LiF-coated anode surface. This ion divergence near the surface is surprisingly large, and accounts for about half the typical 25 mrad final accelerated-beam divergence. The measurements provide constraints for models attempting to explain highly diverging ion emission from thin alkali-halide films in $\sim$10 MV/cm applied fields. [S0031-9007(96)01464-0]

PACS numbers: 52.75.Pv, 41.75.Ak, 52.25.Ya

To date, $\sim$1.5 TW/cm^2 Li^+ ion beams have heated hohlraum targets to 58 eV radiation temperatures, delivering $\sim$20 kJ to the hohlraum in 15 ns on the Particle Beam Fusion Accelerator II (PBFA II) facility at Sandia National Laboratories [1,2]. Further increases in focused beam intensity are needed to produce ignition and gain in an inertial confinement fusion (ICF) hohlraum. The focusability of the ion beam can be quantified by the divergence, the half width at half maximum spread in beam ion velocities transverse (perpendicular) to the direction of beam acceleration divided by the final accelerated beam velocity. The ion beam intensity at focus is inversely proportional to the square of the divergence, so understanding and minimizing the contributions to beam divergence is critical.

Applied-B ion diodes convert pulsed electrical power propagating in magnetically insulated transmission lines into a directed ion beam [3,4]. In the PBFA II diode a $\sim$3 T magnetic field applied parallel to the anode surface inhibits electrons from directly crossing the 1.8 cm anode-cathode (AK) gap when a 10 MV potential difference is present. The Li^+ ions emitted from the LiF-coated anode surface are accelerated across the AK gap, through a virtual cathode of magnetically confined electrons, and on into a gas cell for charge- and current-neutralized transport to a hohlraum at the beam focus. The total divergence of the $\sim$25 ns Li^+ beam is the sum of contributions from the ion source [5], from beam nonuniformities [6], from coupling to electromagnetic fluctuations in the diode AK gap [7,8], and from transport in the gas cell [9].

The beam divergence at the ion source can, in principle, be obtained by measuring ion Doppler broadening parallel to and near the anode surface, as Maron *et al.* [5] have demonstrated on 0.005 TW diodes for carbon and other impurity ions. In practice, emission from Li^+ transitions is not seen in our diodes, and diagnosing the 10^{12}–10^{13} cm^{-3} ion and electron densities in these 20 TW, single-pulse devices is difficult. However, our spectroscopic measurements of Li I $2s$-$2p$ emission in the AK gap reveal the presence of Li atoms having several-keV energies. These energies apparently are acquired near the anode surface by charge exchange (CX) of the Li^+ beam ions on a desorbed impurity layer. In this way, measurements of the Li atoms out in the AK gap with mm-scale spatial resolution allow us to determine the Li^+ beam divergence where the CX events occurred, within 50 μm of the anode ion emission surface. We find that this divergence near the LiF ion source constitutes 10–16 mrad of the typical 25 mrad measured final divergence after 10 MeV beam acceleration and transport [10], indicating that the LiF ion source is a significant contributor to the total divergence, but that other divergence mechanisms must also be investigated. The final ion transverse energy measured in these experiments is about double that required in a 30 MeV ion diode for ICF applications [11].

The ion emission mechanism of thin alkali-halide films subjected to 5–10 MV/cm macroscopic electric fields in not yet understood in detail, but it does not involve the flash-over process creating an anode plasma [12]. This is confirmed by spectroscopic observations that a large electric field is present at the anode surface during ion emission [13], in contrast to a zero-field Child-Langmuir-type ion source. As discussed elsewhere [8,12], scanning electron micrographs of the 1 μm thick LiF film show roughly 10^{10} cm^{-2} densely packed columnar LiF crystallites, and atomic force microscopy of the films gives a characteristic roughness size of less than 30 nm (this does not include the 0.1–1 μm roughness of various stainless steel anode substrates used). It is intriguing that (i) even after accounting for the modest field enhancement due to surface roughness, the surface electric field strength is still far less than the 100–200 MV/cm needed for direct field emission, and (ii)

simple estimates of ion divergence arising from thin-film or substrate surface roughness give near-surface divergence values much smaller than what we find here experimentally [8]. In addition, the ion beam divergence both near the anode surface and after acceleration does not vary systematically with anode substrate roughness over the 0.1–1 μm range tested in our experiments. Theoretical work has argued that the normally insulating LiF becomes a moderate electronic conductor from the flux of multi-MeV electrons that diffuse across the AK gap insulating flux, and this conductivity allows Li^+ ions to be removed from the crystallite tips by field desorption [12]. Longer time scale experiments have shown that pieces of LiF can be pulled off a microneedle at applied fields of about 6–15 MV/cm [14]. Ion emission from fragments of the LiF film may account for the relatively low macroscopic field emission threshold and the large beam divergence at the ion source [8]. Nevertheless, microscopic details of the ion emission remain unknown.

As detailed elsewhere [15], we use an array of fiber optics to collect light from collimated, 2 mm diameter cylindrical lines of sight oriented roughly parallel to and at various distances from the LiF anode surface. This light is transported to multiple remote spectrographs and streaked, intensified, and recorded on film. Each channel records a spectrum from a single line-of-sight position in the AK gap. The entire apparatus has been carefully characterized and absolute sensitivity calibrations are done for each channel after each experiment. The experimental configurations used here recorded data from up to 18 spatial positions with ~1 ns, 1 Å, and 2 mm resolutions.

As shown in Fig. 1, the $2s$-$2p$ emission appears first on the line-of-sight viewing along the anode surface, typically at or a few ns after the ion beam onset. The emission peaks on the near-anode line of sight at about the time the Li^+ beam current peaks, and then peaks and falls in a similar way on each successive line of sight, with a delay and at reduced intensity. These typical intensity data are obtained from multiple-Gaussian fits [16] to 4 ns duration line outs from the digitized film for 7 sequential lines of sight arrayed across the AK gap on a single experiment.

The successive appearance of the $2s$-$2p$ emission at each line of sight indicates propagation of the Li atoms into the AK gap at roughly 50 cm/μs. The intensity decreases with distance from the anode because radiative decay depletes the $2p$-level population. We construct a simple model to obtain the time-dependent velocity. The Li atoms are born near the anode and freely drift away with a distribution $f_\perp(v_\perp)$, where $v_\perp(t)$ is the velocity normal to the anode, while the $2p$-level population radiatively decays to the $2s$ ground level. The measured line-of-sight-averaged $2p$ population density N_{2p} near the anode determines the time-dependent rate of $2p$-atom flux into the AK gap. The Li atom $f_\perp(v_\perp(t))$ and radiative decay determine the subsequent N_{2p} seen on each successive line of sight. Populating the $2p$ level from higher-level Li atoms in the AK gap is negligible until late times because of electric field ionization [17]. Ion impact excitation is a small effect until later in the pulse, and collisional deexcitation is slow because of the low particle density. The atom velocity distribution $f_\perp(v_\perp)$ is unknown, but we have used simple monoenergetic, $f_\perp(v_\perp) = \delta(v_\perp - v_\perp^0)$, or quasimonoenergetic assumptions to obtain good fits to the N_{2p} histories on up to 7 simultaneous line-of-sight data. The motivation for these assumptions will be discussed below. Note that for the monoenergetic assumption, a single time-dependent beam velocity $v_\perp^0$ must fit up to 6 independent measurements. A typical monoenergetic model fit to the measured N_{2p} histories of Fig. 1 is shown in Fig. 2. Within the $\pm 16\%$ 1-sigma relative uncertainty of the sensitivity calibration of each line-of-sight channel, the simple model gives very good fits. The fitted velocities are $v_\perp^0 \sim 50$–70 cm/μs, corresponding to ~10 keV energies, and were constant or slowly decreasing in time. The quasimonoenergetic $f_\perp(v_\perp)$ fits gave similar results.

The Li I distribution of velocities parallel to the anode surface $f_\parallel(v_\parallel)$ can be obtained from the Doppler effect on

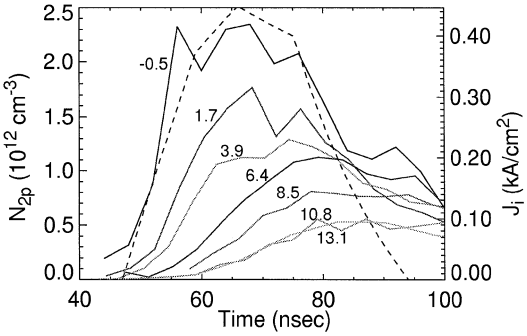

FIG. 1. Li I $2p$ population densities, averaged over the 2 mm diameter lines of sight, at successive anode distances as measured in a single experiment. Distances are from the center of the line of sight to the anode, and are noted in mm for each curve. Dashed curve is Li^+ ion current density J_i.

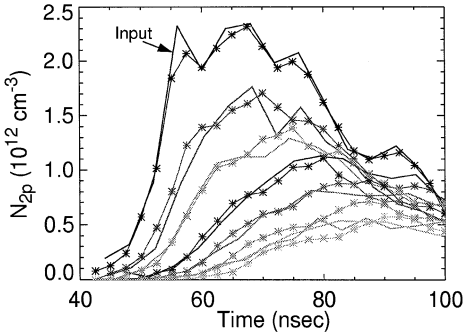

FIG. 2. Measured Li I $2p$ population densities of Fig. 1 (lines) overlaid by model fit (lines with asterisks). The nearest-anode line-of-sight data are the time-dependent input to the fit. A single parameter $v_\perp^0(t)$ gives reasonable agreement on the six successive lines of sight.

the $2s$-$2p$ spectral line profiles. The linewidths rapidly increase within a few ns after appearance to 11–15 Å full width half maximum, and slowly decrease with similar values on successive lines of sight. The Doppler broadening is much greater than the typical 1 Å instrument broadening and the negligible Stark broadening. Opacity broadening of this resonance line has been checked by using a fiber optic to shine blueshifted, 3 Å wide dye laser light into the AK gap to saturate the $2s$-$2p$ transition, while measuring the increase in $2p$ emission in order to set an upper bound on the $2s$ level population. Optical depth of this resonance line for $N_{2s} \sim 5 \times 10^{12}$ cm^{-3} and the 8 cm path is about 1, so opacity broadening is at most a 20% effect. Calculations of the emission pattern in our crossed electric and magnetic fields and line-of-sight orientation [13] show that Zeeman and Stark shifts have a very small effect on the linewidth, the Stark effect producing an overall centroid shift. Another possible line-broadening mechanism is due to gradients of the electric field over the line-of-sight volume or variations in time over the typically 4 ns line-out averaging interval. To evaluate these effects we synthesized $2s$-$2p$ line profiles with varying degrees of Doppler width and electric field gradients. Any physically meaningful gradients we tried could not match the similar spectral linewidths and shifts observed simultaneously on multiple lines of sight, unless the gradient-induced broadening was less than 15% of the observed widths. Thus, the net $2s$-$2p$ Doppler widths correspond to temperatures of 3–6 keV, giving a typical half-width-half-maximum velocity $v_{\parallel}^0$ of 25 cm/μs.

The ~3 keV parallel and ~10 keV perpendicular measured Li atom energies are strong evidence that the atoms arise due to CX of a portion of the accelerating ions on a thin cold-atom layer near the anode surface. We believe this process is nonresonant CX rather than $Li^+ + Li$, based on the fact that, despite the intense MeV electron bombardment of the anode surface, the LiF temperature rise is much too small for the vapor pressure of Li to create sufficient slow Li atoms for resonant CX. Indeed, previous theoretical considerations of the LiF anode coating have argued strongly against any mechanism for prompt Li atom production during the PBFA II power pulse [12]. In addition, measurements of LiF-coated samples from the PBFA II environment have shown that there is at least a monolayer of adsorbed contaminants that can desorb promptly under energetic electron bombardment and anode heating [18]. Note also that the dominant energy of the fast Li atoms is not consistent with resonant CX processes since these should peak at zero energy. In contrast, typical nonresonant CX cross sections $\sigma_{CX}(v_\perp)$ are monotonically increasing with energy in our regime. If the desorbed-layer density $N_L(x)$ does not decrease too rapidly with distance x from the anode across the layer thickness, the increasing CX probability per unit length $dp_{CX}/dx = N_L(x(v_\perp))\sigma_{CX}(v_\perp)$ as a Li^+ ion is accelerated across the impurity neutral layer would make dp_{CX}/dx peak at some maximum $v_\perp$. This could explain why the monoenergetic fast-atom velocity distribution gives such good N_{2p} fits.

We estimate that less than 10% of the Li^+ beam ions undergo CX events in a few desorbed impurity monolayers. The fraction of ions involved in CX events is approximately the neutral flux divided by the ion flux, $3N_{2p}v_\perp^0 e/J_i \approx 0.1$, where the Li^+ current density J_i and N_{2p} are from Fig. 1, and we use calculations of the state-selective energy-dependent CX cross sections [19] indicating that about 1/3 of the CX Li atoms are formed in the $2p$ level. For the number of impurity monolayers, assume the Li^+ ions exchange charge with hydrogen atoms (although the exact desorbed layer composition is not known), giving a cross section at incident speed $v_\perp^0 = 50$ cm/μs of $\sigma_{CX} \sim 2 \times 10^{-17}$ cm^2 [20]. A monolayer corresponds to $n_a \sim 1 \times 10^{15}$ cm^{-2} areal density, so the probability per desorbed monolayer of a Li^+ ion undergoing a CX event is $n_a\sigma_{CX} \approx 1/50$. Equating the flux of Li^+ ions undergoing a CX event with the resulting neutral flux gives $(3N_{2p}v_\perp^0 e)/(n_a\sigma_{CX}J_i) \approx 5$ desorbed monolayers.

The Li atom velocity $v_\perp^0$ can also be used to estimate the CX impurity layer thickness provided the electric field strength is known near the surface. Previous Stark shift measurements [13] showed 10 MV/cm fields near the LiF anode in PBFA II. Early in the pulse, before ion space charge is large, the electric field at the anode is then $E_a \sim 10$ MV/cm, and we estimate the impurity layer thickness as $l \sim \frac{1}{2}m_0(v_\perp^0)^2/(eE_a) \sim 10$ μm. We calculate that even if the anode ion emission were space-charge limited ($E_a = 0$) the layer thickness would be only about 50–60 μm. The fast Li atom velocities $v_\perp^0(t)$ we determine do not typically increase in time, which is perhaps due to the combined temporal variation of the desorbed-layer thickness and of the electric field near the surface. It is interesting that the measured Li^+ beam current density is roughly proportional to the observed $N_{2p}(t)$, as shown in Fig. 1, until the time that the simple model fits start failing. This and the fitted approximately constant fast-atom velocity $v_\perp^0$ indicate a constant CX probability and thus a constant impurity layer areal density, implying that the impurity desorption is more like an impulse rather than a steady process.

The divergence of the Li^+ beam within a few tens of microns of the anode surface may be obtained from the Li atom Doppler broadening a millimeter or more from the surface if the momentum of the lithium atoms resulting from CX events can be related to the momentum of the Li^+ ions. The observed final beam divergence of about 25 mrad at 10 MeV corresponds to 0.8 rad at 10 keV near the anode. At several keV incident energies the charge exchange may be considered a forward-scattering event since angular deflection of the Li^+ ion is far smaller than 0.8 rad [19]. It is possible that a newly created fast Li atom may suffer at most a few collisions with

slow impurity atoms before exiting the CX layer, but these will also be forward-scattering events at our energies [21]. This means that the Li^+ ion velocity distribution is transferred to the CX-generated Li atom distribution, with a geometrical weighting effect for different path lengths in the CX impurity layer. Modeling this geometry effect, we find that for our parameters the Li^+ ion Doppler broadening is about 80% of the value determined from the Li atom Doppler broadening. The Li^+ equivalent divergence near the ion emission source $\Delta\theta_{\rm src}$ may be expressed in terms of the Li atom Doppler width $\Delta\gamma$ as

$$\Delta\theta_{\rm src} = 0.8\,\frac{v_{\|}^0}{c}\sqrt{\frac{M_i c^2}{2eV}} \approx 3.4\,\frac{\Delta\gamma_{\rm \AA}}{\sqrt{V_{MV}}}\,{\rm mrad}\,,$$

where M_i is the Li^+ ion mass and V is the AK gap accelerating potential. Conservatively, the possibility of the small opacity or field-gradient broadening effects discussed above make this expression an upper bound by at most about 20%.

This quantity can be compared with the divergence $\Delta\theta_{\rm total}$ of the accelerated, transported ion beam determined from the size of the final focal spot [22]. On one of the highest-power experiments, the spectroscopically determined divergence near the LiF surface was 15–16 mrad and roughly constant in time, while the final divergence at the time of peak Li^+ power was 22 mrad, at a beam energy of 9.8 MeV. The additional divergence must be acquired by the beam in the AK gap or transport regions, and this additional component should add in quadrature to that near the source. Other experiments with larger $\Delta\theta_{\rm total}$ showed similar $\Delta\theta_{\rm src}$ of 10–16 mrad. Thus the inferred Li^+ transverse ion energy near the source is at most about half that of the accelerated ion beam, and is large enough that this passive thin-film LiF ion source as is cannot meet the high-yield ICF requirement [11] of 11 mrad final divergence at 10 MeV that scales to ICF gain at 35 MeV. We do have an active preformed-plasma ion source that appears to meet this criterion [23]. Within the assumptions of this approach, we have established a novel method for determining the divergence of a high-power Li^+ ion beam within a few tens of microns of the ion emission surface by using spectroscopic measurements of fast-atom properties several millimeters from the surface. The ion emission observation and relatively large angular spread in ion emission velocities near the LiF surface under these high fields are interesting alklai-halide thin-film surface phenomena.

Our thanks to the PBFA II operations crew and D. F. Wenger for technical assistance with the experiments. D. R. Schultz of ORNL kindly provided state-selective Li CX differential cross sections. We are also grateful to M. E. Cuneo, M. P. Desjarlais, T. A. Green, and S. A. Slutz for many useful discussions and to D. L. Cook, R. J. Leeper, and J. P. Quintenz for continuous support and encouragement. This work was supported by the U.S. Department of Energy under Contract No. DE-AC04-94-AL85000.

[1] A. R. Moats *et al.*, Rev. Sci. Instrum. **66**, 743 (1995).
[2] M. S. Derzon *et al.*, Phys. Rev. Lett. **76**, 435 (1996).
[3] S. Humphries, Jr., Nucl. Fusion **20**, 1549 (1980).
[4] D. J. Johnson *et al.*, J. Appl. Phys. **53**, 4579 (1982).
[5] Y. Maron, M. D. Coleman, D. A. Hammer, and H. S. Peng, J. Appl. Phys. **61**, 4781 (1987); Y. Maron *et al.*, Phys. Rev. A **39**, 5842 (1989).
[6] S. A. Slutz, Phys. Fluids B **4**, 2645 (1992).
[7] M. P. Desjarlais *et al.*, Phys. Rev. Lett. **67**, 3094 (1991).
[8] S. A. Slutz *et al.*, Phys. Plasmas **3**, 2175 (1996).
[9] C. L. Olson and J. W. Poukey, in *Proceedings of the 9th International Conference on High Power Particle Beams, Washington, DC, 1992* (National Technical Information Service Report NTIS PB92-206168, Springfield, VA) p. 897.
[10] T. A. Mehlhorn *et al., Proceedings of the 10th International Conference on High Power Particle Beams, San Diego, CA, 1994* (National Technical Information Service Report NTIS PB95-144317, Springfield, VA) p. 53.
[11] R. E. Olson *et al., Proceedings of the 15th IEEE-NPSS Symposium on Fusion Engineering, Hyannis, MA, 1993* (IEEE Service Center, Piscataway, NJ, 1994), p. 189.
[12] T. A. Green *et al.*, Sandia National Laboratories Report No. SAND95-1794. Available from NTIS.
[13] J. E. Bailey *et al.*, Phys. Rev. Lett. **74**, 1771 (1995).
[14] J. A. Panitz, J. Vac. Sci. Technol. B **12**, 2889 (1994); P. R. Schwoebel and J. A. Panitz, J. Appl. Phys. **71**, 2151 (1992).
[15] J. Bailey, A. L. Carlson, R. L. Morrison, and Y. Maron, Rev. Sci. Instrum. **61**, 3075 (1990); J. E. Bailey, A. L. Carlson, and P. Lake, in *Proceedings of the 1994 IEEE International Conference on Plasma Science, Santa Fe, 1994, IEEE Catalog No. 94CH3465-2, p. 133* (IEEE, Piscataway, NJ, 1994).
[16] R. L. Coldwell and G. J. Bamford, *The Theory and Operation of Spectral Analysis Using Robfit* (AIP, New York, 1991).
[17] F. A Ilkov, J. E. Decker, and S. L. Chin, J. Phys. B **25**, 4005 (1992).
[18] M. E. Cuneo *et al.*, in Proceedings of the 10th IEEE Pulsed Power Conference, Albuquerque, NM, 1995 (to be published).
[19] D. R. Schultz (private communication).
[20] J. Van Eck and J. Kistemaker, Physica (Utrecht) **26**, 629 (1960).
[21] A. P. Kalinin *et al.*, Chem. Phys. **85**, 341 (1984).
[22] R. J. Leeper *et al.*, Nucl. Instrum. Methods Phys. Res., Sect. B **40/41**, 973 (1989).
[23] A. B. Filuk *et al.*, in Ref. [9] p. 794.